EDGE ARTICLE

Check for updates

Light-controlled artificial transmembrane signal transduction for 'ON/OFF'-switchable transphosphorylation of an RNA model substrate†

Jinxing Hou,[a] Jiale Guo,[a] Tengfei Yan,[b] Shengda Liu,[b] Mingsong Zang,[a] Liang Wang,[a] Jiayun Xu,[b] Quan Luo, [ID][ac] Tingting Wang*[b] and Junqiu Liu [ID] *[ab]

Inspired by nature, it is of significant importance to design and construct biomimetic signaling systems to mimic natural signal transduction. Herein, we report an azobenzene/α-cyclodextrin (α-CD)-based signal transduction system with three functional modules: a light-responsive headgroup, lipid-anchored group, pro-catalyst tailgroup. The transducer can be inserted into the vesicular membrane to trigger the transmembrane translocation of molecules under the activation of light, forming a ribonuclease-like effector site and leading to the transphosphorylation of the RNA model substrate inside the vesicles. Moreover, the transphosphorylation process can be reversibly turned 'ON/OFF' over multiple cycles by the activation and deactivation of the pro-catalyst. This artificial photo-controlled signal transduction successfully constructs a signal responsive catalysis system across the membrane to utilize light to reversibly control the internal transphosphorylation process of an RNA model substrate, which might provide a new strategy for future design to utilize exogenous signals for implementing endogenous enzyme manipulation and gene regulation.

Introduction

In nature, signal transduction allows the communication of chemical information across cell membranes. It is a prerequisite for numerous important physiological processes such as expression of genes,[1] regulation of metabolism[2] and sustainment of ion homeostasis.[3] Designing artificial systems to simulate the natural signal transduction process is of great significance for understanding the operation principle of cells.[4] Besides artificial channels and carriers,[5,6] some novel artificial signal transduction systems which do not rely on matter exchange have recently represented a significant area of research, because the input signals and output signals of these systems can be chemically unrelated. For instance, Clayden *et al.* described a synthetic signal transduction system in which a conformational change triggered by Cu(II) coordination was used to transmit chemical signals across the membrane.[7] Liu *et al.* proposed an artificial signal system which can control the dimerization of synthetic DNA-based receptors for transmitting

signals.[8] Furthermore, Hunter *et al.* reported a novel membrane-translocation mechanism that does not exist in nature to achieve signal transduction *via* the polar change of the recognition headgroup,[9–11] which provides us with impetus to further mimic many important physiological processes.[12]

It is well known that cells can sense and respond to external signals to control internal catalytic activities through natural signaling pathways.[13] Typically, receptor tyrosine kinases (RTKs)[14,15] composed of two transmembrane proteins can be triggered by dimerization to enhance their kinase activity for catalyzing the phosphorylation of intracellular target proteins when binding to extracellular signals (*e.g.* growth factors). Besides RTKs, G-protein coupled receptors (GPCRs)[16,17] undergo a global conformational change when recognizing the first messenger (*e.g.* neurotransmitters and hormones) to generate a second messenger for recruiting internal enzymes and activating their catalytic activities. These signal responsive catalysis processes across the bilayer are crucial in the (bio)chemical reaction networks of life. Therefore, it is of paramount significance to design an artificial signal transduction system that utilizes external signaling to control internal catalytic behavior of an enclosed membrane structure, which might provide a powerful tool for biosensing technology and synthetic biology.

Light, which is noninvasive, remote and wavelength-tunable, plays a central role in life science and medical science.[18–20] Stimuli such as ligand recognition,[9] pH change[10] and redox[11] have been used to design and construct signal transduction models, while light-gated signaling systems as an ideal pathway

[a]State Key Laboratory of Supramolecular Structure and Materials, College of Chemistry, Jilin University, 2699 Qianjin Road, Changchun 130012, China. E-mail: junqiuliu@jlu.edu.cn

[b]College of Material, Chemistry and Chemical Engineering, Hangzhou Normal University, Hangzhou 311121, China

[c]Key Laboratory for Molecular Enzymology and Engineering of Ministry of Education, School of Life Sciences, Jilin University, Changchun 130012, China

† Electronic supplementary information (ESI) available. See DOI: https://doi.org/10.1039/d2sc06701c

are rarely reported.[21,22] Azobenzene, one of the most classic molecular photoswitches, will undergo a conformational conversion from a *trans* isomer to a *cis* isomer upon ∼365 nm ultraviolet (UV) light irradiation.[23] More importantly, *trans*-azobenzene can not only be complexed with α-CD to change its physicochemical properties (*e.g.* water solubility), but also isomerizes under UV illumination to detach from the cavity of α-CD, which provides us with a powerful candidate for the construction of light-gated signal transduction.

Here, a photoswitchable signal transduction molecule consisting of three functional elements was designed: (I) *trans*-azobenzene/α-CD (*t*Azo/α-CD) as the light-responsive headgroup for responding to external signaling inputs; (II) lithocholic acid (LA) as the lipid-anchored group that can trap the signaling molecule in the vesicular membrane; (III) 1,4,7-triazacyclonane (TACN) as the pro-catalyst tailgroup for Zn^{2+}-coordination to form ribonuclease-like catalysis sites.[24] Besides, the system includes 2-hydroxypropyl-4-nitrophenylphosphate (HPNP) as the RNA model substrate, which is a well-known molecule to simulate the RNA phosphodiester structure.[25,26] As shown in Scheme 1, this transduction process should involve three sequential steps. First, driven by the preference of the water-soluble *t*Azo/α-CD headgroup to lie in the aqueous phase, the *t*Azo-LA-TACN/α-CD system is embedded in the membrane in the 'OFF' state, where the TACN unit is trapped in the lipid phase to prevent its Zn^{2+}-coordination. Upon UV irradiation, *t*Azo-LA-TACN/α-CD could be dissociated to generate and release *c*Azo-LA-TACN due to the isomerization of *trans*-azobenzene to *cis*-azobenzene. Subsequently, the resulting *c*Azo-LA-TACN moves into the vesicular membrane, and meanwhile the TACN unit is forced to enter the water phase inside the vesicle. Finally, the TACN unit catches a Zn^{2+} to form a ribonuclease-like site for hydrolyzing RNA model substrate — HPNP, whose transphosphorylation allows releasing a UV-absorbing output signal of *p*-nitrophenol (PNP, $\lambda_{abs} = 405$ nm).

Results and discussion

Molecular photoisomerization behavior

The detailed synthesis of *t*Azo-LA-TACN is depicted in Schemes S1–S3.† The photoisomerization behavior of *t*Azo-LA-TACN was investigated in methanol-d_4 (2 mM) by ^{1}H NMR spectroscopy. As shown in Fig. 1a, the new proton signals (*i.e.*, H$_a^*$, H$_b^*$, H$_c^*$, H$_d^*$ and H$_e^*$) of *c*Azo-LA-TACN were observed after 365 nm UV-irradiating for 120 s, which demonstrated the isomerization of *t*Azo-LA-TACN to *c*Azo-LA-TACN. Subsequent visible light irradiation for 30 s led to a decrease in the new proton signal intensity (H$_a^*$, H$_b^*$, H$_c^*$, H$_d^*$ and H$_e^*$) and an increase in the original proton signal intensity (H$_a$, H$_b$, H$_c$, H$_d$ and H$_e$), indicating the conformational recovery from *c*Azo-LA-TACN to *t*Azo-LA-TACN using visible light. Furthermore, based on the integral ratio changes of the new proton signal intensity and the original proton signal intensity, the conversion efficiency was calculated to be 82% and 85% for *t*Azo-LA-TACN to *c*Azo-LA-TACN and *c*Azo-LA-TACN to *t*Azo-LA-TACN, respectively. The reversible photoisomerization behavior was further demonstrated by the evolution of UV absorption spectroscopy (Fig. S1†).
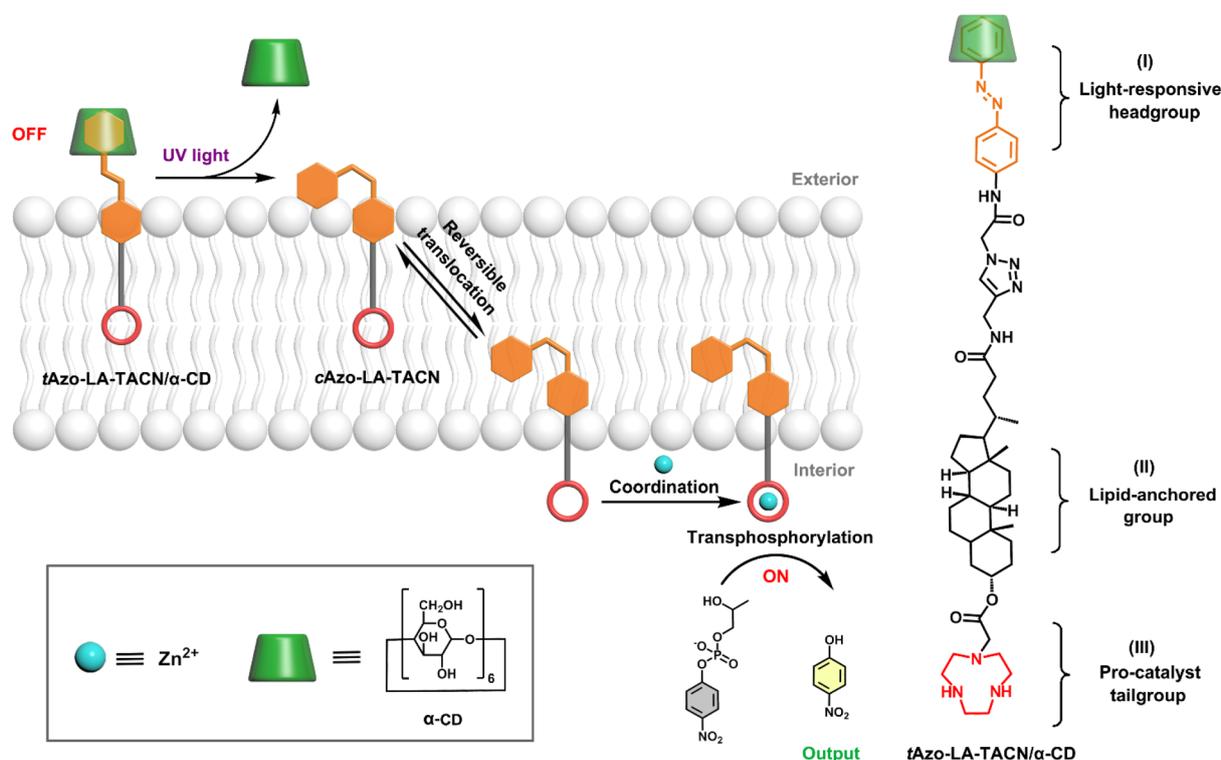
Scheme 1 Schematic representation of light–responsive transmembrane signal transduction for transphosphorylation of an RNA model substrate and the molecular structure of Azo–LA–TACN/α-CD.
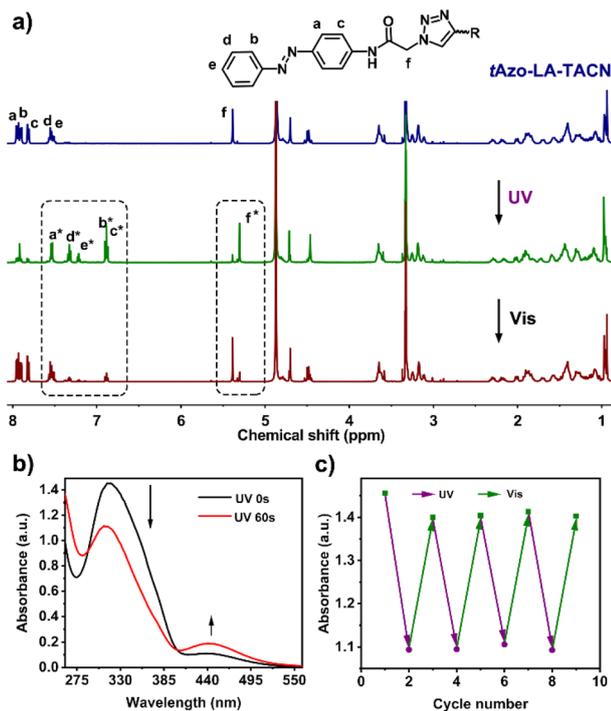
a)

Fig. 1 (a) ^{1}HNMR spectra (500 MHz) of *t*Azo-LA-TACN before and after UV irradiation (365 nm, 5.0 mW cm^{-2}, 120 s), and subsequent visible light (530 nm, 5.0 mW cm^{-2}, 30 s) in methanol-d_4 at 2.0 mM. The superscript "*" shows that the peak is assigned to *c*Azo-LA-TACN. (b) UV-vis spectra of *t*Azo-LA-TACN/α-CD photoisomerization before and after UV irradiation (365 nm, 5.0 mW cm^{-2}, 60 s) in DMSO/H$_2$O (1/99, v/v) at 0.1 mM. (c) The reversible switching of *t*Azo-LA-TACN/α-CD upon alternative irradiation of UV (365 nm, 5.0 mW cm^{-2}, 60 s) and visible light (530 nm, 5.0 mW cm^{-2}, 30 s).

Next, the host–guest complexation properties and the photoisomerization behavior of *t*Azo-LA-TACN/α-CD were explored. When adding α-CD, the UV-vis absorption peak of *t*Azo-LA-TACN was blueshifted from 323 nm to 310 nm (Fig. S2a†) and the proton signals underwent a downfield shift (Fig. S2b†), indicating the complexation of *t*Azo-LA-TACN with α-CD. Furthermore, the association constant of *t*Azo-LA-TACN with α-CD was assessed to be (3435 ± 130) M^{-1} by ^{1}H NMR spectroscopic titrations[27,28] (Fig. S3†), indicating that α-CD could bind to *t*Azo-LA-TACN to form stable host–guest complexes in the aqueous solution, which provided the basis for the photoisomerization of *t*Azo-LA-TACN/α-CD and transmembrane signaling experiments. In addition, the critical assembling concentration (CAC)[29,30] of *t*Azo-LA-TACN/α-CD was measured to be 21.2 μM (Fig. S4†), which was used to indicate the proper concentration of *t*Azo-LA-TACN/α-CD in the transmembrane signal transduction for avoiding molecular aggregation. We also explored the photoisomerization behavior of *t*Azo-LA-TACN in the presence of α-CD by UV absorption spectroscopy. Irradiation of UV light onto *t*Azo-LA-TACN/α-CD from 0 s to 60 s resulted in a gradual decrease of the π–π* band at 310 nm and a gradual increase of the n–π* band at 442 nm, and the fluctuation can be restored upon visible light irradiation for 30 s (Fig. 1a and S5†). More importantly, the interconversion between *t*Azo-LA-TACN and *c*Azo-LA-TACN can be achieved for

at least four cycles upon alternative irradiation with UV and visible light (Fig. 1b).

We also studied the binding of *c*Azo-LA-TACN to Zn^{2+} for the transphosphorylation activity of HPNP in the absence of liposomes. The methylene proton signals of the TACN unit exhibited a downfield-shift after the addition of Zn^{2+}, confirming the binding of the TACN unit to Zn^{2+} (Fig. S6†). As the model substrate of RNA, HPNP can be transphosphorylated to release PNP, which can induce a constant increase in UV-absorbance when monitoring at 405 nm from 0 to 600 s. As shown in Fig. S7,† both the groups containing *c*Azo-LA-TACN or Zn^{2+} exhibited a low transphosphorylation efficiency, while the simultaneous addition of *c*Azo-LA-TACN and Zn^{2+} to a HEPES buffer solution of HPNP triggered a dramatic increase in UV absorbance at 405 nm, indicating the ability of *c*Azo-LA-TACN to catalyze the transphosphorylation of HPNP after Zn^{2+}-coordination.

Molecular membrane interaction. Prior to photoswitchable transmembrane signal transduction, we first probed the insertion of the transducer into the lipid membranes by confocal laser scanning microscopy (CLSM) on DOPC/DOPE giant unilamellar vesicles (GUVs). Given the non-fluorescence of *t*Azo-LA-TACN/α-CD, rhodamine B modified α-CD (α-CD-RhB) was utilized to visualize the transducer instead of α-CD. The GUVs premixed with a membrane dye (DiO) were incubated with *t*Azo-LA-TACN/α-CD-RhB, and then the excess dye and transducer were washed off for CLSM measurement. As seen in Fig. 2a, the red fluorescence signal from *t*Azo-LA-TACN/α-CD-RhB was observed around the vesicular membranes and highly overlapped with the green signal from the premixed DiO dye. Differential scanning calorimetry (DSC) analysis was also used to verify the ability of the transducer to integrate into the lipid bilayer. The DSC analysis showed that the addition of *t*Azo-LA-TACN/α-CD to the vesicles induced a broadening of lipid phase transition, revealing the insertion of the transducer rather than
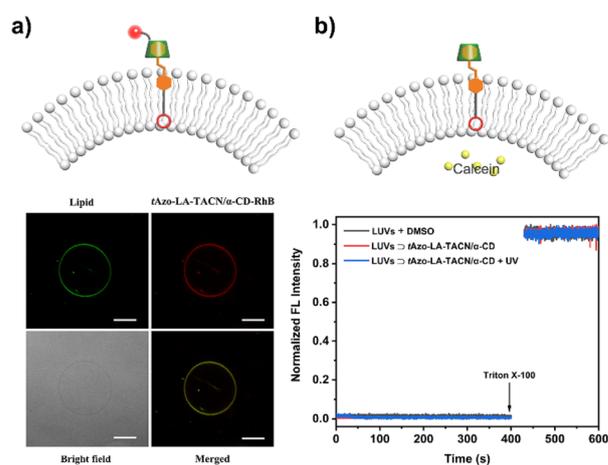

Fig. 2 (a) Confocal fluorescence images of DiO-labelled DOPC/DOPE GUVs (green) after incubation with *t*Azo-LA-TACN/α-CD-RhB (red). Scale bar, 10 μm. (b) Calcein release assays of DOPC/DOPE LUVs (100 mM calcein, 20 mM HEPES, pH = 8.0) in the absence (black) of *t*Azo-LA-TACN/α-CD and in the presence of *t*Azo-LA-TACN/α-CD without (red) or with (blue) UV irradiation (365 nm, 5.0 mW cm^{-2}, 120 s).

surface absorption (Fig. S8†). In addition, we found that the transducer can also undergo reversible conformational conversion in the membrane as in solution (Fig. S9†), which was shown as a *cis*-isomer and *trans*-isomer corresponding to UV and visible light irradiation, respectively.

To explore the stability of the vesicular membrane, the calcein release experiment and dynamic light scattering (DLS) analysis were performed. It was found that the addition of *t*Azo-LA-TACN/α-CD to the LUVs and subsequent UV irradiation caused an almost negligible release of encapsulated calcein (Fig. 2b) and slight changes in LUV size (Fig. S10†), verifying that the transducer and its isomerization did not destabilize the membrane integrity. All the results provided a powerful prerequisite for light-gated transmembrane signal transduction.

Transmembrane signal transduction. To carry out transmembrane signal transduction assay, large unilamellar vesicles (LUVs) loaded with $Zn(NO_3)_2$ and HPNP were prepared using a DOPC/DOPE lipid at a molar ratio of 4 : 1 (6.9 mg/1.6 mg). The LUVs were confirmed to have an average diameter of 200 nm by employing dynamic light scattering (DLS) analysis (Fig. S11a†) and a lipid concentration of 1.2 mM (Fig. S11b†). In the transmembrane experiments, the concentration of *t*Azo-LA-TACN/α-CD was 7.5 μM, which was below its critical assembling concentration (CAC, 21.2 μM) to avoid the self-assembly of amphiphilic *t*Azo-LA-TACN/α-CD in water.

The UV-vis kinetics results of signal transduction triggered by *in situ* UV illumination are depicted in Fig. 3a. A control of (Zn^{2+}/HPNP)-contained LUVs in the absence of *t*Azo-LA-TACN/α-CD showed a very low transphosphorylation activity after addition of DMSO due to the background hydrolysis of HPNP (Fig. 3a, black data), and similar activity was observed in the LUVs without *t*Azo-LA-TACN/α-CD before and after UV irradiation (Fig S13†). The (Zn^{2+}/HPNP)-contained LUVs loaded with *t*Azo-LA-TACN/α-CD, *i.e.*, the 'OFF' state of the system, exhibited a slight increase in UV absorbance (Fig. 3a, red data). Interestingly, after 'OFF' for 50 s, the signaling system can be further switched into the 'ON' state by UV irradiation for 120 s to provoke a significant increase in the transphosphorylation rate (Fig. 3a, green data), indicating the generation of *c*Azo-LA-TACN and its translocation towards intravesicular water for Zn^{2+}-coordination. In a reaction time of 600 s, the transphosphorylation ratio of the 'ON' state exhibited a 7-fold amplification compared to that of the 'OFF' state. Besides PNP, sodium cyclic phosphate (cyP), as another transphosphorylation product of HPNP, can also serve as an output signal to monitor the transduction process by ^{31}P NMR spectroscopy. Fig. 3b shows that UV irradiation for LUVs in the 'OFF' state led to a decrease in ^{31}P NMR resonances at $\delta_{HPNP} = -6.0$ ppm and the appearance of new ^{31}P NMR resonances at $\delta_{cyP} = 14.5$ ppm, demonstrating the generation of cyP and the formation of the 'ON' state. Additionally, the generation of PNP and cyP was confirmed by electrospray ionization mass spectra (ESI-MS). From ESI-MS we could simultaneously find the mass peak of $[PNP + H]^+$ and $[cyP + Na]^+$ on the same sample taken from the 'ON' state (Fig. 3c), which was consistent with UV-vis kinetics assay and ^{31}P NMR study. In addition, we performed the signal transduction assay with variable concentrations of Zn^{2+}, showing that the transphosphorylation rate increased with a higher concentration (Fig. 4), thus strongly indicating that Zn^{2+} was also an indispensable factor in the light signaling system.
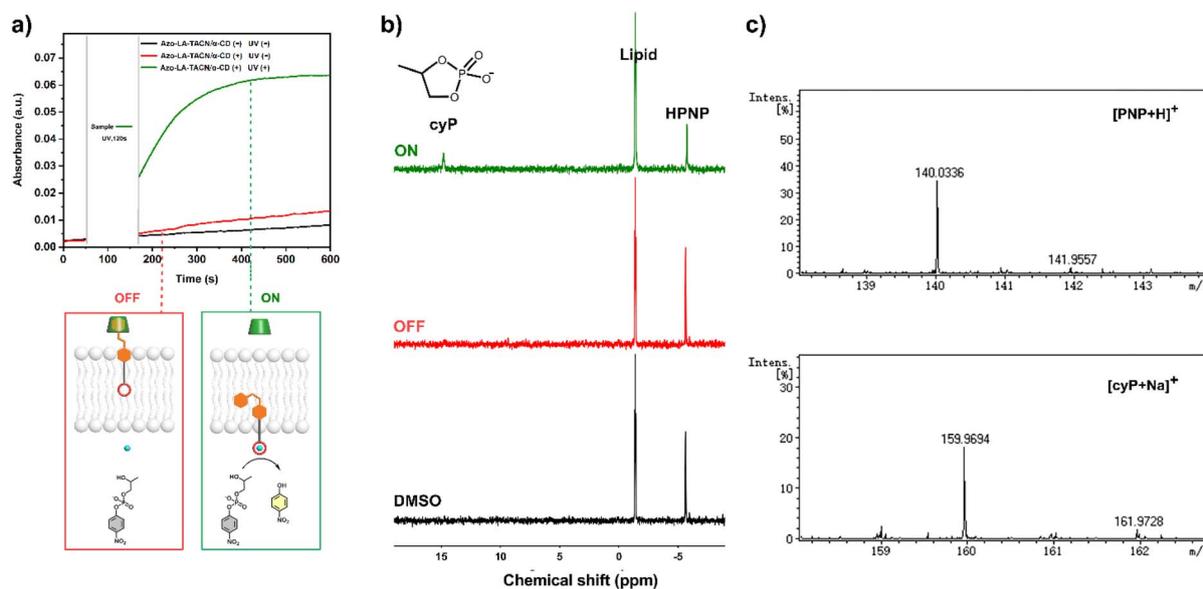

Fig. 3 Light-triggered signal transmembrane transduction experiments for transphosphorylation of HPNP. (a) Time-dependent UV-vis spectra at 405 nm of DOPC/DOPE LUVs (1.75 mM HPNP, 0.25 mM Zn^{2+}, 20 mM HEPES, pH = 8.0) in the absence (black) of *t*Azo-LA-TACN/α-CD and in the presence of *t*Azo-LA-TACN/α-CD (7.5 μM *t*Azo-LA-TACN and 0.5 mM α-CD) without (red) or with (green) UV irradiation (365 nm, 5.0 mW cm^{-2}, 120 s). (b) ^{31}P NMR spectra of DOPC/DOPE LUVs in the absence (black) of *t*Azo-LA-TACN/α-CD and in the presence of *t*Azo-LA-TACN/α-CD (7.5 μM *t*Azo-LA-TACN and 0.5 mM α-CD) without (red) or with (green) UV irradiation (365 nm, 5.0 mW cm^{-2}, 120 s) in DMSO-d_6. (c) Mass spectra of $[PNP + H]^+$ and $[cyP + Na]^+$ taken from LUVs in the presence of *t*Azo-LA-TACN/α-CD (7.5 μM *t*Azo-LA-TACN and 0.5 mM α-CD) with UV irradiation (365 nm, 5.0 mW cm^{-2}, 120 s).
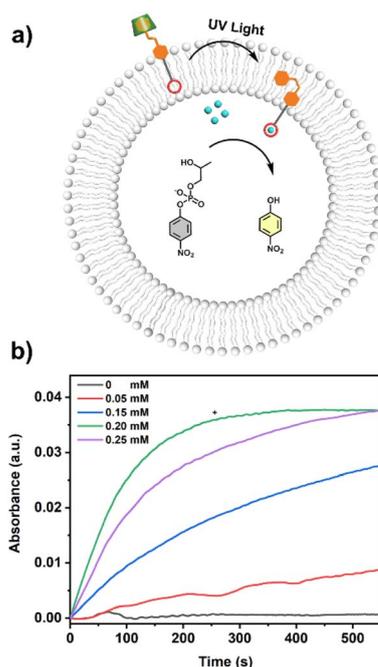
Fig. 4 (a) Schematic representation of light-responsive signal transduction based on LUVs loaded with varied concentrations of Zn^{2+}. (b) Time-dependent UV-vis spectra at 405 nm of LUVs (1.75 mM HPNP, 20 mM HEPES, pH = 8.0) loaded with varied concentrations of Zn^{2+} (0 mM, 0.05 mM, 0.15 mM, 0.20 mM and 0.25 mM) in the absence (−) or presence (+) of tAzo-LA-TACN/α-CD (7.5 μM tAzo-LA-TACN and 0.5 mM α-CD).

Furthermore, to verify the importance of the chemical structure of tAzo-LA-TACN/α-CD in boosting the signal transduction, we performed control experiments using two sub-modules of tAzo-LA-TACN/α-CD (i.e., tAzo-LA/α-CD and TACN). First, we found that there was no marked increase in the transphosphorylation rate with addition of tAzo-LA/α-CD alone to the extra-vesicular solution and subsequent UV irradiation, indicating the necessity of TACN to trigger intra-vesicular transphosphorylation activity (Fig. S14,† red data). Then we probed the same assay by adding both TACN and tAzo-LA/α-CD to the extra-vesicular solution, in which a negligible transphosphorylation acceleration was measured after UV light irradiation (Fig. S14,† black data). The results show that TACN and tAzo-LA/α-CD must be covalently linked to benefit from its transmembrane translocation.

To enrich the multi-responsiveness of the transmembrane signaling system, competitive supramolecular recognition was also used to trigger the signal transduction based on the tAzo-LA-TACN/β-CD system. As shown in Fig. S15b,† the addition of 1-adamantanamine hydrochloride (ADA) to the extra-vesicular solution can trigger the translocation of tAzo-LA-TACN across the membrane for Zn^{2+} coordination, leading to the transphosphorylation of HPNP. Moreover, the ON/OFF switches of the transphosphorylation behavior can be reversibly switched by alternately adding ADA and β-CD (Fig. S15c†). The ADA-triggered signal transduction indicated that the system can also

respond to the chemical signals on one side of the lipid membrane to transmit information.

Reversible 'ON/OFF' switches of signal transduction

The conformational change and recovery of transmembrane signaling proteins (e.g. G-protein coupled receptors) usually correspond to the active and inactive states of signal transduction.[31] Therefore, achieving reversible control of artificial systems by conformational conversion is of importance for understanding the natural signal transduction process. Herein, the 'ON/OFF' switches of the tAzo-LA-TACN/α-CD signaling system were also achieved by UV and visible light-controlled conformational conversion. As illustrated in Fig. 5, tAzo-LA-TACN/α-CD was added to the (Zn^{2+}/HPNP)-containing LUVs to form the initial 'OFF' state, where a negligible signal increase was observed in a reaction time of 50 s. Subsequently, the signaling activity was activated by UV irradiation for 120 s that triggered a dramatic increase in the transphosphorylation rate. After visible light irradiation for 30 s for converting cAzo-LA-TACN to tAzo-LA-TACN, the signaling process was switched back to 'OFF' resulting from the complexation of tAzo-LA-TACN with α-CD again. Interestingly, UV irradiation for 240 s for the LUVs induced a second increase in the HPNP transphosphorylation rate, indicating that the signal transduction system was recovered to 'ON'. These results demonstrated that the tAzo-LA-TACN/α-CD system can be reversibly regulated by light-triggered conformational conversion to control 'ON/OFF'-switchable transphosphorylation behavior, analogous to natural transmembrane proteins to control the 'ON/OFF' of the signaling process through reversible allostery.
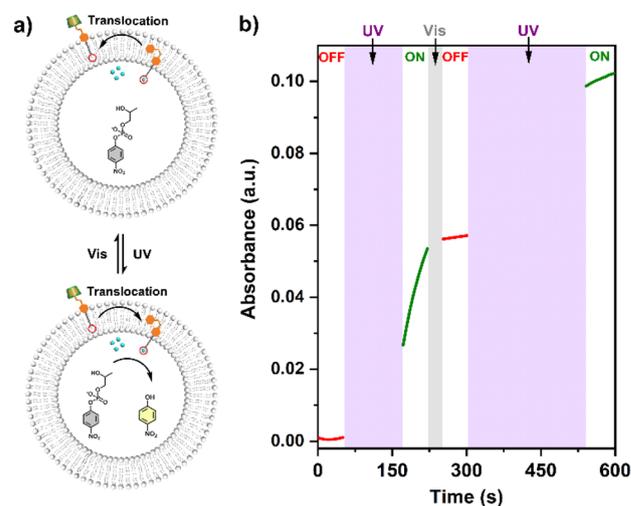

Fig. 5 (a) Schematic representation of the reversible light-responsive signal transduction for 'ON/OFF' switches of transphosphorylation by alternatively irradiating UV and visible light. (b) Time-dependent UV-vis spectra at 405 nm of LUVs (1.75 mM HPNP, 0.25 mM Zn^{2+}, 20 mM HEPES, pH = 8.0) in the presence of tAzo-LA-TACN/α-CD (7.5 μM tAzo-LA-TACN and 0.5 mM α-CD) to switch transphosphorylation 'ON' after 120 s-UV irradiation, switch 'OFF' after 30 s-vis irradiation, and switch 'ON' again after 240 s-UV irradiation.

Conclusions

In conclusion, a photoswitchable signal transduction system to convert external light signals into the internal catalysis process for 'ON/OFF'-switchable transphosphorylation of a RNA model substrate was successfully constructed based on the *t*Azo-LA-TACN/α-CD system. *In situ* irradiation of UV to LUVs can trigger the *trans* to *cis* isomerization of this transducer and the dissociation of *t*Azo-LA-TACN/α-CD, which induced molecular translocation across the membrane to activate the pro-catalyst *via* Zn^{2+}-coordination, ultimately resulting in a 7-fold enhancement in the transphosphorylation signal. The transphosphorylation activity can be activated and deactivated over multiple cycles by the UV/vis-induced conformational changes of *t*Azo-LA-TACN, indicating that the light strategy was successfully used as a powerful means for constructing reversible artificial signal transduction. Our study fabricated a modular signaling system to implement the signal responsive catalysis of an RNA model substrate across the membrane, which provided the basis for future design to achieve endogenous enzyme manipulation for gene regulation in vesicles or even in actual cells. In addition, the modular design allows it to be retrofitted to any system of interest by changing the pro-catalyst tailgroup for application in optogenetics and photopharmacology.

Data availability

The experimental methods and datasets that support this article are available in the ESI.†

Author contributions

J. H. synthesized and characterized Azo-LA-TACN. J. H. and J. G. performed the UV-vis and fluorescence experiments. M. Z. and T. Y. carried out the NMR assays. All authors contributed to the analysis of the results. J. H., T. W. and J. L. wrote and revised the manuscript.

Conflicts of interest

There are no conflicts to declare.

Acknowledgements

Notes and references

1 A. H. Brivanlou and J. E. Darnell, *Science*, 2002, **295**, 813–818.

2 A. Latoscha, D. J. Drexler, M. M. Al-Bassam, A. M. Bandera, V. Kaever, K. C. Findlay, G. Witte and N. Tschowri, *Proc. Natl. Acad. Sci. U.S.A.*, 2020, **117**, 7392–7400.

3 P. Kakanj, B. Moussian, S. Grönke, V. Bustos, S. A. Eming, L. Partridge and M. Leptin, *Nat. Commun.*, 2016, **7**, 12972.

4 C. Maffeo, S. Bhattacharya, J. Yoo, D. Wells and A. Aksimentiev, *Chem. Rev.*, 2012, **112**, 6250–6284.

5 W.-L. Huang, X.-D. Wang, Y.-F. Ao, Q.-Q. Wang and D.-X. Wang, *J. Am. Chem. Soc.*, 2020, **142**, 13273–13277.

6 A. J. Scott, A. Niitsu, H. T. Kratochvil, E. J. M. Lang, J. T. Sengel, W. M. Dawson, K. R. Mahendran, M. Mravic, A. R. Thomson, R. L. Brady, L. Liu, A. J. Mulholland, H. Bayley, W. F. DeGrado, M. I. Wallace and D. N. Woolfson, *Nat. Chem.*, 2021, **13**, 643–650.

7 F. G. A. Lister, B. A. F. Le Bailly, S. J. Webb and J. Clayden, *Nat. Chem.*, 2017, **9**, 420–425.

8 H. Chen, L. Zhou, C. Li, X. He, J. Huang, X. Yang, H. Shi, K. Wang and J. Liu, *Chem. Sci.*, 2021, **12**, 8224–8230.

9 M. J. Langton, N. H. Williams and C. A. Hunter, *J. Am. Chem. Soc.*, 2017, **139**, 6461–6466.

10 M. J. Langton, F. Keymeulen, M. Ciaccia, N. H. Williams and C. A. Hunter, *Nat. Chem.*, 2017, **9**, 426–430.

11 L. Trevisan, I. Kocsis and C. A. Hunter, *Chem. Commun.*, 2021, **57**, 2196–2198.

12 J. Hou, X. Jiang, F. Yang, L. Wang, T. Yan, S. Liu, J. Xu, C. Hou, Q. Luo and J. Liu, *Chem. Commun.*, 2022, **58**, 5725–5728.

13 I. J. Uings, *Mol. Pathol.*, 2000, **53**, 295–299.

14 M. A. Lemmon and J. Schlessinger, *Cell*, 2010, **141**, 1117–1134.

15 M. D. Paul and K. Hristova, *Chem. Rev.*, 2019, **119**, 5881–5921.

16 C. D. Hanlon and D. J. Andrew, *J. Cell Sci.*, 2015, jcs.175158.

17 D. Hilger, M. Masureel and B. K. Kobilka, *Nat. Struct. Mol. Biol.*, 2018, **25**, 4–12.

18 E. A. Widder, *Science*, 2010, **328**, 704–708.

19 P. C. Donthamsetti, J. Broichhagen, V. Vyklicky, C. Stanley, Z. Fu, M. Visel, J. L. Levitz, J. A. Javitch, D. Trauner and E. Y. Isacoff, *J. Am. Chem. Soc.*, 2019, **141**, 11522–11530.

20 P. Donthamsetti, D. B. Konrad, B. Hetzler, Z. Fu, D. Trauner and E. Y. Isacoff, *J. Am. Chem. Soc.*, 2021, **143**, 8951–8956.

21 M. De Poli, W. Zawodny, O. Quinonero, M. Lorch, S. J. Webb and J. Clayden, *Science*, 2016, **352**, 575–580.

22 H. Yang, S. Du, Z. Ye, X. Wang, Z. Yan, C. Lian, C. Bao and L. Zhu, *Chem. Sci.*, 2022, **13**, 2487–2494.

23 H. Fliegl, A. Köhn, C. Hättig and R. Ahlrichs, *J. Am. Chem. Soc.*, 2003, **125**, 9821–9827.

24 F. Manea, F. B. Houillon, L. Pasquato and P. Scrimin, *Angew. Chem.*, 2004, **116**, 6291–6295.

25 S. Neri, S. Garcia Martin, C. Pezzato and L. J. Prins, *J. Am. Chem. Soc.*, 2017, **139**, 1794–1797.

26 C. Z. -J. Ren, P. Solís Muñana, J. Dupont, S. S. Zhou and J. L. -Y. Chen, *Angew. Chem., Int. Ed.*, 2019, **58**, 15254–15258.

27 P. Thordarson, *Chem. Soc. Rev.*, 2011, **40**, 1305–1323.

28 J. Royes, C. Courtine, C. Lorenzo, N. Lauth-de Viguerie, A.-F. Mingotaud and V. Pimienta, *J. Org. Chem.*, 2020, **85**, 6509–6518.

29 R. Dong, B. Zhu, Y. Zhou, D. Yan and X. Zhu, *Angew. Chem., Int. Ed.*, 2012, **51**, 11633–11637.

30 Q. Yan, J. Wang, Y. Yin and J. Yuan, *Angew. Chem., Int. Ed.*, 2013, **52**, 5070–5073.

31 J. Kniazeff, *J. Neurosci.*, 2004, **24**, 370–377.